

Effect of cover cracking on reliability of corroded reinforced concrete structures

Hua-Peng Chen^{*1} and Jaya Nepal^{2a}

¹Department of Engineering Science, University of Greenwich at Medway, Chatham Maritime, Kent ME4 4TB, U.K.

²School of Architecture, Computing & Engineering, University of East London, London E16 2RD, U.K.

(Received July 25, 2017, Revised August 10, 2017, Accepted August 19, 2017)

Abstract. The reliability of reinforced concrete structures is frequently compromised by the deterioration caused by reinforcement corrosion. Evaluating the effect caused by reinforcement corrosion on structural behaviour of corrosion damaged concrete structures is essential for effective and reliable infrastructure management. In lifecycle management of corrosion affected reinforced concrete structures, it is difficult to correctly assess the lifecycle performance due to the uncertainties associated with structural resistance deterioration. This paper presents a stochastic deterioration modelling approach to evaluate the performance deterioration of corroded concrete structures during their service life. The flexural strength deterioration is analytically predicted on the basis of bond strength evolution caused by reinforcement corrosion, which is examined by the experimental and field data available. An assessment criterion is defined to evaluate the flexural strength deterioration for the time-dependent reliability analysis. The results from the worked examples show that the proposed approach is capable of evaluating the structural reliability of corrosion damaged concrete structures.

Keywords: lifecycle performance; stochastic deterioration modelling; structural reliability; reinforcement corrosion; residual strength

1. Introduction

Reinforcement corrosion has been identified as the main cause of the deterioration of reinforced concrete (RC) structures worldwide. The major source of reinforcement corrosion can be either due to the environment pollution (i.e. carbonation) or the ingress of chloride ion in the RC structures exposed to deicing salt or marine environment, but the latter is the major factor (Tilly *et al.* 2007, Chen and Nepal 2016, Chen 2016). The costs associated with managing these corrosion damaged RC structures are tremendous. In Europe, about 50% of its annual construction budget has been spent on refurbishment and repair of existing structures (Tilly *et al.* 2007). In addition to these direct costs, there is significant portion of indirect costs such as traffic delay and loss of life and property. Therefore, the deterioration of RC structures caused by reinforcement corrosion has significant influence on infrastructure management and is of greater challenge both technically and economically. Corrosion of steel reinforcement affects the performance of existing RC structures in various ways such as loss of rebar area, cracking in concrete cover and degradation of bond strength between rebar and concrete (Coronelli 2002, Nepal and Chen 2015, Yalciner *et al.* 2012). Bond strength acting at

the rebar surface has the interaction mechanism that enables the force transfer between rebar and the surrounding concrete. Hence, bond strength maintains the composite action in RC structures to ensure the structures operate safely. When composite action is disrupted, load carrying capacity of the RC structures is also affected (Wang and Liu 2010, Shang *et al.* 2012, Mangat and Elgarf 1999, Azad *et al.* 2010). The understanding of the effects of corrosion on the structural behaviour of deteriorated RC structures would allow asset managers to make effective and reliable decisions related to the inspection, repair, strengthening, replacement and demolition of these RC structures. This can ultimately help in achieving the goal of sustainable infrastructure management.

The performance degradation of RC structures caused by reinforcement corrosion is time-variant and uncertain as well in nature. Uncertainties associated with the resistance degradation make it difficult to accurately predict the lifecycle performance of these structures. Time-dependent reliability analysis provides a framework and quantitative tool for the condition assessment of RC structures suffering from reinforcement corrosion. This can further help in making decision regarding optimal allocation of resources for maintenance, repair and replacement. During the past decade, time-dependent structural reliability analysis has been widely utilised to evaluate probability of failure over time and optimise maintenance strategy during service life (Yi *et al.* 2016, Chen and Alani 2012, Van Noortwijk 2009). However, limited efforts have been made in relationship between cracking in the concrete cover surface and residual load bearing capacity and its effect on the structural reliability of corrosion damaged RC structures.

*Corresponding author, Professor

E-mail: h.chen@gre.ac.uk

^aLecturer

E-mail: j.nepal@uel.ac.uk

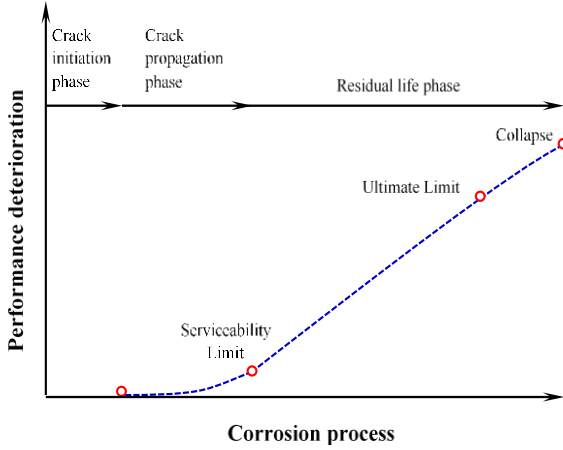


Fig. 1 Schematic representation of performance deterioration of corrosion affected reinforced concrete structures

This paper presents a method for time-dependent reliability analysis and lifecycle performance assessment of corrosion affected RC structures. Analytical models are provided to evaluate the evolution of flexural strength deterioration due to corrosion induced concrete cover cracking. In order to model the progression of structural resistance deterioration during the life cycle, a stochastic process such as gamma process is adopted to take uncertainties in modelling into account. The time-dependent reliability analysis is then applied to evaluate the probability of failure of the RC structure by using the associated ultimate limit state analysis. Finally, a case study of Ullasund Bridge together with a numerical example of a RC beam is used to demonstrate the applicability of the proposed approach.

2. Performance deterioration caused by corrosion

In lifecycle modelling of corrosion damaged RC structures serving in aggressive environments, the effect of corrosion on the resistance of the RC structures can be illustrated in Fig. 1 (Chen and Alani 2013). In this paper, the lifecycle of a RC structure subjected to reinforcement corrosion is defined as the period for the completion of construction to the collapse of the structure. As observed from Fig. 1, in the crack initiation phase, structural resistance remains almost the same as the original capacity. In the crack propagation phase, structural resistance deterioration accumulates gradually until reaching the serviceability limit. The structural resistance deterioration rate accelerates in the residual life phase, leading to the collapse of the structure. This phenomenon of the structural resistance degradation in the whole life of RC structures can be basically contributed from three main factors: i.e., reinforcement corrosion, cover cracking and strength deterioration.

2.1 Reinforcement corrosion

The ingress of chlorides through the concrete cover

deactivates the natural protective oxide layer formed around the reinforcements. Once the protective layer is disturbed, corrosion initiates at the rebar surfaces. In general, there are two types of corrosion process, uniform corrosion and pitting corrosion (Zhang *et al.* 2010, Khan *et al.* 2014). The reduction in radius of original rebar R_b can be estimated from $R_{bx}=R_b-\alpha_p x/2$ (Vidal *et al.* 2004), in which α_p is an attack penetration factor indicating localised corrosion at the earlier stage when $4<\alpha_p<8$ and homogeneous corrosion at later stage when $\alpha_p=2$, and x is the associated corrosion depth. Based on the study carried out in Zhang *et al.* (2010), corrosion is typically uniform in the later stage of corroded RC structures. Therefore, in this paper corrosion is considered as uniform, since residual strengths are mainly affected by reinforcement corrosion in later stage. The assumption of uniform corrosion is often utilised in investigations of the effect of reinforcement corrosion on concrete performance, such as in studies Coronelli (2002) and Wang and Liu (2004). The corresponding corrosion level X_p is defined as the ratio of the mass loss ΔM_s , or area loss ΔA_b of the corroded rebar to the original mass M_o or area A_b of the rebar, namely

$$X_p = \frac{\Delta M_s}{M_o} = \frac{\Delta A_b}{A_b} = 1 - \frac{R_{bx}^2}{R_b^2} \quad (1)$$

Once the mass loss due to corrosion is known, the volume of the rust product V_r per unit length of the rebar can be estimated from $V_r=\gamma_{vol}X_p\pi R_b^2$, in which γ_{vol} is the volume ratio of corrosion product formed to its parent metal, generally ranging between 1.8 to 6.4. The corresponding volume increase per unit length of the rebar ΔV can be obtained by deducting the volume of steel consumed from the volume of the rust product formed. Then the uniform displacement at the bond interface u_{bx} , generated by expansive corrosion product, is given by

$$u_{bx} = \frac{\Delta V}{2\pi R_b} = \frac{1}{2}(\gamma_{vol} - 1)R_b X_p \quad (2)$$

2.2 Corrosion induced cover cracking

The evolution of cracks in concrete cover is discussed in the analytical investigations by Chen and Alani (2013) and Chen and Xiao (2012), where the equivalent crack width w as defined as the cumulated crack width over the cover surface. The intact cover concrete is treated as elastic in nature and the cracked concrete due to tensile hoop stress cause by rebar corrosion is considered as anisotropic. From the anisotropic property and the bilinear softening law of the cracked concrete defined in CEB-FIP (1990), the normalised cumulative crack width W_{bx} at the rebar surface R_b is obtained in Chen and Xiao (2012), and written here as

$$W_{bx} = \frac{1}{b(l_o - R_b)} \left(\frac{E}{f_t} u_{bx} - aR_b \right) \quad (3)$$

where a and b are the coefficients of bilinear softening curve which depends on the stage of cracking in the cover

concrete; E is the effective modulus of elasticity of the concrete defined as $E=E_c/(1+\theta_c)$ in which E_c is the modulus of elasticity of concrete and θ_c is the creep coefficient; f_t is the maximum tensile strength of concrete at onset of cracking; l_o is the material constant given by $l_o=n_c l_{ch}/2\pi b$ in which l_{ch} is the characteristic length defined as $l_{ch}=EG_f/f_t^2$ where G_f is fracture energy of the concrete, f_t is the tensile strength of the concrete and n_c is the total number of cracks. Typical value of total crack number in thick walled cylinder model is approximately three or four from the experimental data. Similarly, the cumulative crack width over the concrete cover surface w_{cx} can also be obtained by considering boundary conditions and ignoring the Poisson's effect associated with the hoop strain of the completely cracked concrete (Chen and Xiao 2012), expressed here as

$$w_{cx} = \left(\frac{G_f}{f_t} \right) \times \frac{\frac{E}{f_t} u_{bx} - a [R_b + R_c (l_o - R_c) (l_o - R_b) \cdot \delta(R_c, R_b)]}{b (l_o - R_b) [1 - R_c (l_o - R_c) \cdot \delta(R_c, R_b)]} \quad (4)$$

where R_c is radii of the concrete cover surface and $\delta(R_c, R_b)$ is the crack factor associated with the material properties and radial distance r , defined as

$$\delta(R_c, R_b) = \frac{R_c - R_b}{l_o (l_o - R_c) (l_o - R_b)} + \frac{1}{l_o^2} \ln \frac{R_c |l_o - R_b|}{R_b |l_o - R_c|} \quad (5)$$

2.3 Corrosion induced residual strength deterioration

Corrosion of rebar affects the bond properties between rebar and the surrounding concrete by changing the shape and angle of the ribs of deformed rebar (Coronelli and Gambarova 2000, Law *et al.* 2011). It also influences the mechanical interlocking and confinement between rebar and the surrounding concrete by reducing adhesion and frictional force caused by the accumulation of corrosion products and cracking in the concrete cover. By considering these effects, an analytical model to evaluate the ultimate bond strength of corroded reinforcement was proposed by Chen and Nepal (2015) by modifying the original model provided by Coronelli (2002). From the modified model, the ultimate bond strength T_{ubx} is obtained from the total contribution of three types of stress acting at the bond interface at certain corrosion level can be evaluated from three contributions, i.e., adhesion stress T_{adx} , confinement stress T_{cnfx} and corrosion stress T_{corr} , namely

$$T_{ubx} = T_{adx} + T_{cnfx} + T_{corr} \quad (6)$$

The adhesion stress T_{adx} acting between rebar and surrounding concrete is given by

$$T_{adx} = \frac{n_r A_{rx} f_{coh} [\cot \delta_o + \tan(\delta_o + \varphi)]}{2\pi R_{bx} S_r} \quad (7)$$

where n_r is the number of transverse ribs at a section; $A_{rx}=2\pi R_{bx} h_{rx}$ is the reduced rib area in plane at right angle to rebar axis in which $h_{rx}=0.14R_{bx}$ is the reduced rib height of the rebar due to corrosion; $S_r=1.2R_b$ is the rib spacing

(Wang and Liu 2004); $f_{coh}=2-10(x-x_c)$ is the adhesion strength coefficient in which x_c is the corrosion depth corresponding to the through cracking of the concrete cover and can be obtained once X_p^c is known (Chen and Nepal 2015); $\tan(\delta_o+\varphi)$ can be estimated from $1.57-0.785x$ in which δ_o is the orientation of the rib usually taken as 45° and φ is the angle of friction between rebar and concrete.

The confinement stress T_{cnfx} contributed by the surrounding cracked concrete and stirrup is given by

$$T_{cnfx} = k_{cnfx} P_{cnfx} \quad (8)$$

where $k_{cnfx}=0.8n_r \tan(\delta_o+\varphi)/\pi$ is the coefficient of confinement stress for crescent shaped rebar and P_{cnfx} is the confinement pressure. In confined concrete, the confinement pressure is defined as the total contribution of cracked concrete $P_{cnfx,c}$ and the stirrups $P_{cnfx,st}$, expressed here as

$$P_{cnfx} = P_{cnfx,c} + P_{cnfx,st} \\ = \frac{C}{R_{bx}} \times f_t \frac{D_a (w_u - w_{bx})}{w_u (D_a + k_c w_{bx})} + \frac{n_{st} A_{st}}{2R_{bx} S_{st}} \times E_{st} \sqrt{\frac{a_2 w_{bx}^2}{\alpha_{st}^2 D_{st}^2} + \frac{a_1 w_{bx}}{\alpha_{st} D_{st}} + a_0} \quad (9)$$

where C is the concrete cover depth; $w_{bx}=G_f W_{bx}/f_t$ is actual crack width at the rebar surface; w_u is the cohesive critical crack width which depends on the concrete strength, fracture energy and maximum aggregate size (Chen and Nepal 2015); k_c is the constant taken as 167; A_{st} is the cross-section area of stirrup leg with diameter of D_{st} ; n_{st} is the number of stirrup legs and S_{st} is the spacing of stirrups; E_{st} is the modulus of elasticity of steel; D_a is maximum aggregate size; α_{st} is the shape factor of stirrup taken as 2; α_2 , α_1 and α_0 are the coefficients related to the simplified trilateral local bond-slip law of the stirrups, given in Giuriani *et al.* (1991).

The ultimate bond strength T_{corr} contributed by the corrosion pressure is defined as

$$T_{corr} = \mu_x P_{corr} \quad (10)$$

in which μ_x is the coefficient of the friction between the corroded rebar and the cracked concrete given by $0.37-0.26(x-x_c)$, and P_{corr} is the corrosion pressure or the radial stress acting at the bond interface, expressed by Chen and Xiao (2012) as

$$P_{corr} = \frac{f_t}{1-\vartheta^2} \left[(1+\vartheta\sqrt{\beta_{bx}})(a-bW_{bx}) + \frac{\xi_{corr}}{(l_o-R_b)} \frac{b}{R_b} + \vartheta\sqrt{\beta_{bx}} b l_o \frac{W_{bx}}{R_b} \right] \quad (11)$$

where ϑ is the Poisson's ratio, ξ_{corr} is the corrosion factor determined from two boundary conditions of the boundary-value problem, depending on the phase of crack development in the concrete, and β_{bx} is the stiffness reduction factor associated with the cracked concrete.

To consider the effect of bond strength degradation on evaluating the deterioration of flexural strength of corroded RC beams, a typical cross section of doubly reinforced RC beam, as shown in Fig. 2, is now considered. The strain and stress distributions across beam section under initial un-

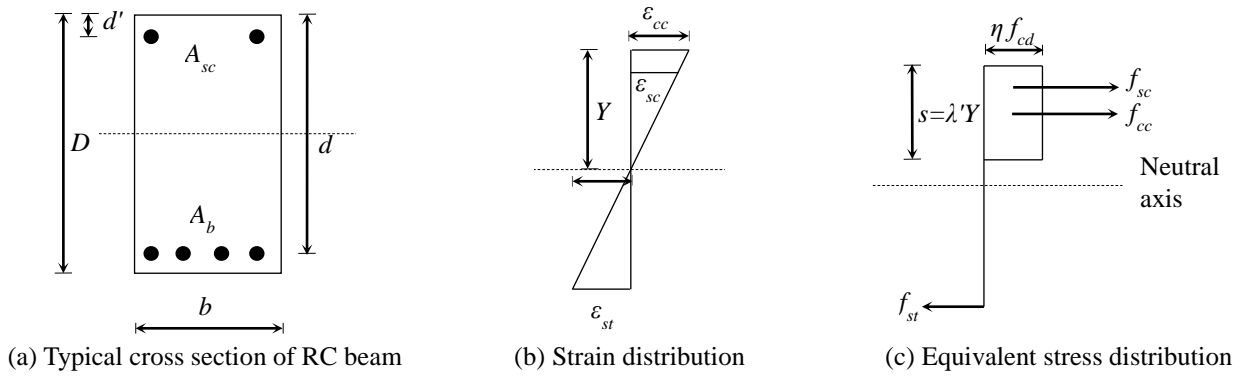


Fig. 2 Flexural analysis of a RC beam section

corroded condition of rebar are shown in Figs. 2(b) and 2(c), respectively, as given by Eurocode 2 (2004). The symbols used in Fig. 2 are defined as: b =width of beam; D =overall depth of the beam; d =effective depth of beam; d' =the distance from centroid of the compression steel rebar to edge of the compression fibre; A_b =initial area of un-corroded tensile steel rebar; A_{sc} =initial area of un-corroded compression rebar with diameter of D_{sc} ; $\epsilon_{cc}=0.0035$ is ultimate strain of concrete; ϵ_{st} =strain of tensile rebar; ϵ_{sc} =the strain of compression rebar; Y =neutral axis depth from the edge of compression zone; f_{st} =tensile stress acting at the centroid of tensile steel; $f_{cd}=\alpha_{cc}f_{ck}/\gamma_c$ is the design strength of the concrete in which α_{cc} is the constants taken as 0.85 for $f_{ck}\leq 50$ MPa, in which f_{ck} is the characteristic compressive strength of the concrete and γ_c =partial factor of safety of the concrete taken as 1.5; s is the equivalent compression zone given by $s=\lambda'Y$; η and λ' are the coefficients taken as 1 and 0.8 for $f_{ck}\leq 50$ MPa. In this study, concrete compressive strength of $f_{ck}\leq 50$ MPa is considered.

In intact condition without rebar corrosion, the ultimate bond strength ($T_{ub,rqd}$) and corresponding development length (l_d) required to prevent anchorage failure are given, respectively,

$$T_{ub,rqd} = \frac{f_{yd}R_b}{2l_d}, \quad l_d = \alpha_{bd} \frac{R_b f_{yd}}{2f_{bd}} \quad (12a,b)$$

where f_{yd} is the design strength of tensile steel rebar given by f_{yk}/γ_s in which f_{yk} is the characteristic tensile strength and $\gamma_s=1.15$ is the partial factor of safety of the steel rebar, respectively; f_{bd} is design bond strength obtained from $f_{bd}=0.315f_{ck}^{0.67}$ for concrete strength $f_{ck}\leq 50$ MPa and rebar diameter $D_b\leq 32$ mm; and α_{bd} is the coefficient depending on many factors including the shape of anchorage, types of confinement provided by the stirrups and concrete cover.

During the progress of reinforcement corrosion, when existing bond strength is sufficient to prevent RC beam from bond failure, the flexural capacity of the RC beam can be obtained by the conventional method based on compatibility condition. In the case of corroded RC beam, when ultimate bond strength is insufficient to prevent anchorage failure, the tensile force generated in the corroded tensile steel can be expressed as

$$f_{stx} = 2n_b\pi R_{bx}l_d T_{ubx} \quad (13)$$

where n_b is the number of the bottom tensile steel.

In the case of un-corroded perfectly bonded beam, strain compatibility condition exists, as defined in design code. But the strain compatibility of a RC beam with corroded reinforcement shift to new compatibility condition and can be considered between un-bonded and bonded condition. Assuming the deformation of concrete is mainly due to plastic deformation occurring within the plastic equivalent region L_{eq} , new strain compatibility of the corroded RC beam is given by Wang and Liu (2010), expressed here as

$$\frac{\epsilon_{stx}}{\epsilon_{ccx}} = g_x \frac{d_x - Y_x}{Y_x}, \quad \frac{\epsilon_{scx}}{\epsilon_{ccx}} = g_x \frac{Y_x - d'_x}{Y_x} \quad (14a,b)$$

where the plastic equivalent region is defined as $L_{eq}=9.3Y_x$ (Au and Du 2004). Parameters in Eq. (14) are defined as: ϵ_{ccx} is ultimate strain of concrete; ϵ_{stx} and ϵ_{scx} are strains of tensile steel and compression steel, respectively; Y_x is the neutral axis depth from the edge of compression zone; d_x is the effective depth of beam, and d'_x is the distance from the centroid of the compression steel to edge of the compressive fibre at corrosion level X_p ; and g_x is the interpolation factor which can be obtained by considering the bond strength value of perfectly bonded and un-bonded condition of the RC beam. Consequently, strain acting at steel rebar is given by bonded and un-bonded condition of the RC beam. Consequently, strain acting at steel rebar is given by

$$\epsilon_{stx} = \frac{f_{stx}}{A_{bx}E_{st}} \quad (15)$$

in which A_{bx} is the reduced area of tensile steel due to corrosion. During the corrosion process, anchorage failure may occur at any stage of yielding of steel and concrete. These yielding stages can be determined by satisfying the limiting values of ϵ_{stx} , ϵ_{ccx} and ϵ_{scx} , as given by Eurocode 2. Generally, when tensile rebar reaches its yielding stage, compressive rebar should also reach its yielding stage. In this study, yielding of tensile rebar is only considered. In order to consider this condition of anchorage failure corresponding to yielding stages of compressive fibre and tensile fibre, three cases are discussed as follows.

Case 1: $\epsilon_{stx}\leq 0.002$ and $\epsilon_{ccx}\leq 0.0035$

During corrosion process, when anchorage failure occurs before yielding of the tensile rebar and the concrete

(i.e., $\varepsilon_{stx} \leq 0.002$ and $\varepsilon_{ccx} \leq 0.0035$), the tensile stress acting along the corroded rebar f_{stx} is governed by the bond strength and hence can be evaluated from Eq. (13). By utilising the concept given by Cairns and Zhao (1993), the corroded RC beam follows the condition of equilibrium of resultant tensile and compressive forces acting at the beam section, and the neutral axis depth Y_x is obtained from

$$Y_x = \frac{f_{stx} - f_{scx}}{\eta \lambda f_{cd} b} \quad (16)$$

where $f_s = f_{ydx} A_{scx}$ is the compressive force acting at the centroid of compression steel in which A_{scx} is the area of the corroded compression steel; $f_{ydx} = (1 - 0.5X_p)f_{yd}$ is the residual yield strength of corroded steel rebar corresponding to corrosion level X_p (Du *et al.* 2005). By taking moment at the centroid of the tensile rebar, the residual flexural strength of corroded RC beam M_{ux} can be evaluated from

$$M_{ux} = f_{ccx} (d_x - 0.4Y_x) + f_{scx} (d_x - d_x') \quad (17)$$

Case 2: $\varepsilon_{stx} > 0.002$ and $\varepsilon_{ccx} \leq 0.0035$

In this case yielding of steel occurs before the anchorage failure (i.e., $\varepsilon_{stx} > 0.002$ and $\varepsilon_{ccx} > 0.0035$), and tensile force is governed by the residual yield strength of the corroded rebar f_{ydx} and is obtained from $f_{stx} = f_{ydx} A_{bx}$. From equilibrium of forces, Y_x in Eq. (16) can be obtained by using the tensile force f_{stx} . Once Y_x is available, the corresponding flexural strength is determined from Eq. (17).

Case 3: $\varepsilon_{stx} > 0.002$ and $\varepsilon_{ccx} > 0.0035$

When both the tensile rebar and the concrete yield before anchorage failure (i.e., $\varepsilon_{stx} > 0.002$ and $\varepsilon_{ccx} > 0.0035$), the strain of steel rebar will be governed by the yielding of the concrete. By using $\varepsilon_{ccx} = \varepsilon_{cc} = 0.0035$, the strain of steel rebar ε_{stx} can be obtained from Eq. (14a). The corresponding tensile stress f_{stx} and the neutral axis depth Y_x are then evaluated from Eqs. (15) and (16), respectively. Finally, the corresponding flexural strength of corroded rebar M_{ux} is determined from Eq. (17).

3. Structural reliability analysis

The gamma process is a stochastic process with independent non-negative increments having a gamma distribution with a given average of deterioration rate (Van Noortwijk 2009). Structural resistance degradation caused by reinforcement corrosion is a continuous and non-negative phenomenon. Therefore, the gamma process is suitable for the stochastic modelling of structural resistance deterioration in corrosion affected RC structures during their lifecycle, and is adopted in this study for stochastic performance deterioration modelling. In the gamma process deterioration model, cumulative resistance deterioration J is considered as a random quantity with the gamma distribution, and has shape parameter $\eta_x > 0$ and scale parameter $\lambda > 0$.

The probability density function of this random quantity J , i.e., the structural resistance during the lifecycle at time t and at corrosion level $X_p (X_p > 0)$, can be expressed as

$$f_{J_x}(J) = Ga(J, \eta_x, \lambda) = \begin{cases} \frac{\lambda^{\eta_x}}{\Gamma(\eta_x)} J^{\eta_x-1} e^{-\lambda J}, & \text{for } J \geq 0 \\ 0, & \text{elsewhere} \end{cases} \quad (18)$$

where $\Gamma(\eta_x) = \int_0^{\infty} v^{\eta_x-1} e^{-v} dv$ is the gamma function for

shape parameter $\eta_x > 0$. The scale parameter λ can be estimated from statistical estimation methods such as a Maximum Likelihood Method by maximizing the logarithm of the likelihood function of the increment of the parameter (Van Noortwijk 2009).

The average flexural strength deterioration J_x can be determined by the ratio of decrease in flexural strength to the initial flexural strength of the RC beam, given by $J_x = 1 - M_{ux}/M_{uo}$. The shape function η_x is then estimated from $\eta_x = \lambda J_x$. Assuming J_L as the maximum allowable limit of the structural deterioration, from the definition of probability of failure and by integrating probability density function given in Eq. (18), the lifetime distribution of probability of failure is given by

$$P_f = P_r[J_x \geq J_L] = \int_{J=J_L}^{\infty} f_{J_x}(J) dJ = \frac{\Gamma(\eta_x, J_L \lambda)}{\Gamma(\eta_x)} \quad (19)$$

where $\Gamma(\eta, z) = \int_{v=z}^{\infty} v^{\eta-1} e^{-v} dv$ is the incomplete gamma

function for $z \geq 0$ and $\eta > 0$. The allowable structural deterioration limit J_L may vary in accordance with the requirements given by asset managers.

4. Worked examples

First, in order to obtain the better understanding of the bond behaviour of corroding rebar, a case study is undertaken here to demonstrate the applicability of the proposed model for evaluating bond strength deterioration of corroded RC structures. The field data of the Ullasund Bridge, Norway, published by Horryngmoe *et al.* (2007), are considered in this study. The Ullasund Bridge was demolished in 1998, only after 29 years of service in harsh environments. From the pieces of concrete collected from the demolished Ullasund Bridge, a total number of 22 cubic specimens with dimensions of 150 mm × 150 mm × 150 mm and single ribbed rebar of diameter 25 mm were prepared for investigations. The yield strength of the rebar was measured as 400 MPa and the compressive strength of the concrete was 40.3 MPa. Bond strength of each specimen was evaluated by pull-out test and the corresponding corrosion level was determined by sandblasting method. Due to lack of details in situ measured material properties, some material properties required for this analytical model are assumed such as Poisson's ratio $\nu = 0.18$, creep coefficient $\theta_c = 2.0$, density of steel $\rho_s = 7850 \text{ kg/m}^3$ and the volume ratio of the corrosion products is taken as $\gamma_{vol} = 2.0$ (Shang *et al.* 2012, Chen and Alani 2013). A typical value of corrosion current density of $1 \text{ } \mu\text{A/cm}^2$ is considered,

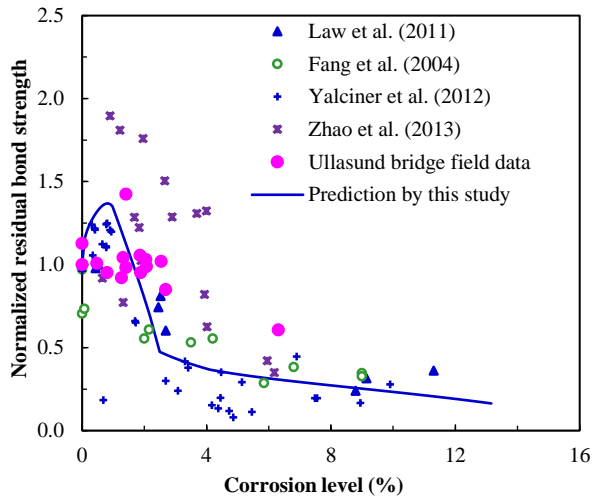


Fig. 3 Normalised residual bond strength versus corrosion level, compared with available field test data of Ullasund Bridge and experimental test results available from various sources

representing nominal amount of mean annual current density measured in field structures (Broomfield 1997). In this study, four cracks in the concrete cover are estimated from the crack band model, and crack width in the concrete cover is represented by the equivalent crack width, as defined in Khan *et al.* (2014). The equivalent critical crack width $w_{cr}=0.2$ mm and ultimate crack width $w_u=1.6$ mm are obtained from CEB-FIP (1990) for the corresponding concrete compressive strength and the adopted maximum aggregate size $D_a=16$ mm. Other parameters such as concrete tensile strength $f_t=4.6$ MPa and modulus of elasticity of the concrete $E_c=37.1$ GPa are estimated from Eurocode 2 (2004).

The predicted results of residual bond strength as a function of corrosion level (X_p) in percentage are shown in Fig. 3 and are compared with the field data of the Ullasund Bridge. In Fig. 3, the normalised residual bond strength is defined as the ratio of the ultimate bond strength of corroded rebar (T_{ubx}) over the ultimate bond strength of original rebar (T_{ubo}). The ultimate bond strength of original rebar is evaluated from Eq. 6, where the corrosion level (X_p) is taken as zero. The predicted results for residual bond strength are in good agreement with the field data. The analytical prediction by this study shows that at the low corrosion level (<1%) there is slight increase in bond strength, but further increase in corrosion leads to significant reduction in bond strength, as observed in the experimental studies. The predicted bond strength after the corrosion level of 2.5% is slightly lower than field data. This may be due to the difference between the material properties of the concrete assumed in the present model and the actual material properties of the Ullasund Bridge. The discrepancy may be also due to the complexity of the reinforcement corrosion and cover cracking mechanism in reality. In addition, the predicted results are compared with the published experimental data of unconfined concrete available from literature, such as Fang *et al.* (2004), Law *et al.* (2011), Yalciner *et al.* (2012) and Zhao *et al.* (2013). In general the bond strength deterioration observed in

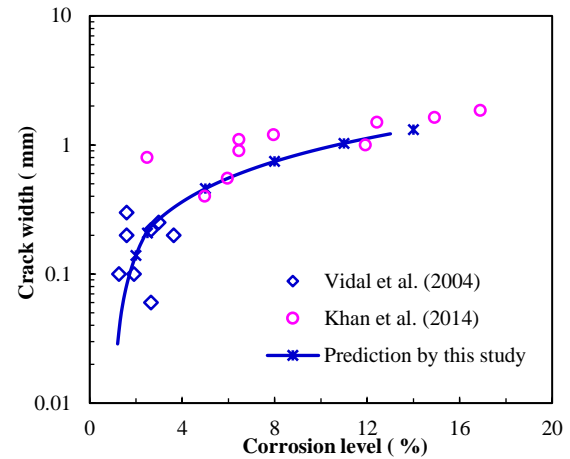


Fig. 4 Equivalent cover surface crack width versus corrosion level, compared with available experimental data from natural corrosion tests in Vidal *et al.* (2004) and Khan *et al.* (2014)

laboratory experimental studies is close to that reported in the field study of Ullasund Bridge, which clearly indicates that the bond strength of RC structures exposed in aggressive environment is seriously affected by reinforcement corrosion.

The results in Fig. 4 show the analytically predicted equivalent cover surface crack width as a function of corrosion level in percentage. The predicted results are then compared with published experimental investigations in natural corrosive environments obtained from Khan *et al.* (2014) and Vidal *et al.* (2004). It can be seen from Figure 4 that the predicted crack width increases as reinforcement corrosion level increases, agreeing well with the referred experimental results. At corrosion level of about 1.5%, concrete cover is thoroughly cracked and the crack width at the cover surface continuously increases with further progress of corrosion.

In order to demonstrate the applicability of the proposed approach in evaluating the structural reliability of corrosion damaged RC structure, a simply supported RC beam of 5 m span is now utilised with a cross section shown in Fig. 2(a). The beam is doubly reinforced with the cross-sectional width $b=300$ mm and effective depth $d=560$ mm, subject to mean annual corrosion current per unit length $i_{cor}=1$ $\mu\text{A}/\text{cm}^2$. Four steel bars with diameter $D_b=20$ mm are provided as the tensile reinforcement and two bars of diameter $D_{sc}=16$ mm as the compressive reinforcement, with clear cover thickness $C=40$ mm along with the stirrup of diameter $D_{st}=6$ mm at spacing of 100 mm. The original reinforcing steel has yield strength $f_{yk}=460$ MPa. The concrete has a characteristic compressive strength $f_{ck}=40$ MPa, and the corresponding concrete properties such as tensile strength and modulus of elasticity are estimated from Eurocode 2 (2004). The ultimate cohesive crack widths required for this study are obtained from CEB-FIP (1990) for maximum aggregate size of 20 mm. Other mechanical properties of concrete are assumed to be the same as those adopted for Ullasund Bridges.

The predicted results from the proposed method are

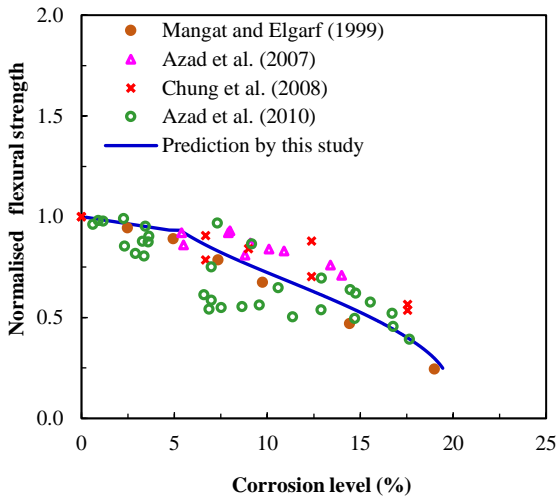


Fig. 5 Normalised residual flexural strength versus corrosion level, compared with available experimental test results

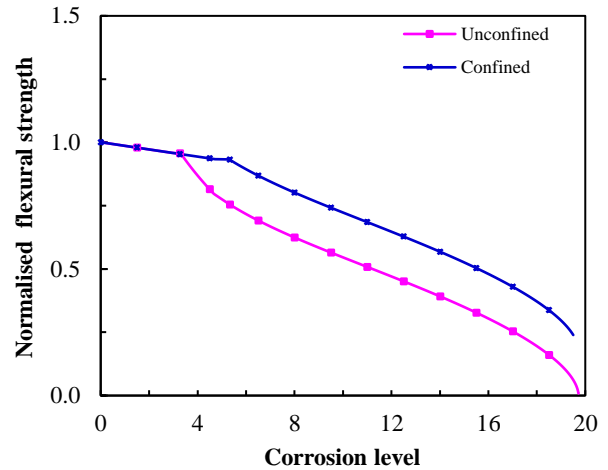


Fig. 7 Normalised residual flexural strength versus corrosion level for confined and unconfined concrete

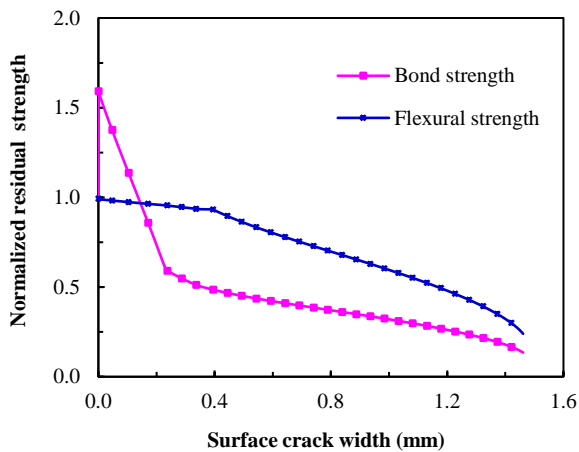


Fig. 6 Normalised residual flexural strength and bond strength versus cover surface crack width

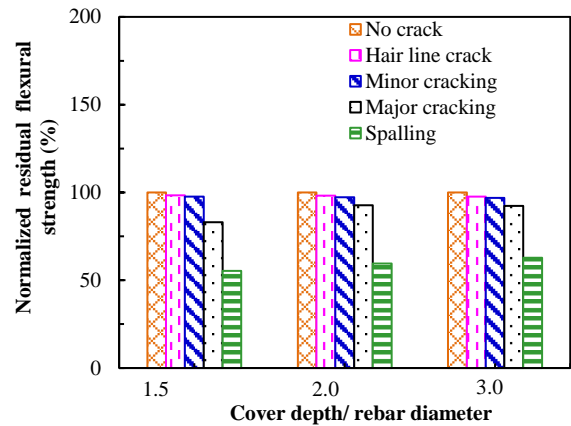


Fig. 8 Normalised residual flexural strength versus cover surface crack defects at different concrete cover depths

plotted in Fig. 5 as a function of corrosion level in percentage and compared with the published experiment data obtained from various sources such as Mangat and Elgarf (1999), Azad *et al.* (2010), Azad *et al.* (2007) and Chung *et al.* (2008). In Fig. 5, the residual load capacity is represented by the normalised flexural capacity, which is calculated by dividing the residual flexural capacity of corroded element by the capacity of the non-corroded element. The results predicted by the present study shows that before the critical point (i.e., where the severe reduction of flexural strength takes place), there is the negligible reduction in flexural strength. However, after the critical point, significant reduction of residual flexural strength occurs, agreeing well with the experimental test results from various sources. The reduction in flexural strength is due to the significant reduction in bond strength, which is required to prevent beam from bond failure. Some discrepancies in critical point can be observed, which could be due to larger confinement stress generated by the cover concrete and the stirrups, and also may be due to the development length sufficient for yielding of the corroded

tension reinforcement before bond failure.

Fig. 6 shows the results of normalised bond and flexural strength versus equivalent cover surface crack width. Both flexural and bond strength of the RC beam continuously decreases with the increase of crack width at the concrete cover surface. Moreover, the results also indicate that bond strength is more affected by cover surface cracking than the flexural strength.

The results in Fig. 7 show the residual flexural strength behaviour of confined and unconfined concrete as function of corrosion level. The results show that the critical point of corrosion is relatively lower in unconfined concrete than in confined concrete. Furthermore, the flexural strength deterioration is also relatively less in confined concrete. This is due to the increase in confinement provided by the stirrups in confined concrete.

Fig. 8 shows the effect of cover surface defects on the residual flexural strength for different concrete cover depths to rebar diameter ratios (C/D_b). Here the hair line crack is defined as crack width ≤ 0.05 mm, minor cracking as 0.05-0.1 mm, major cracking as 0.1-0.4 mm and spalling as 0.4-1.0 mm. At hairline crack stage, residual flexural strength generally remains the same as that in the intact stage for all three cases of concrete cover depths. With further growth of

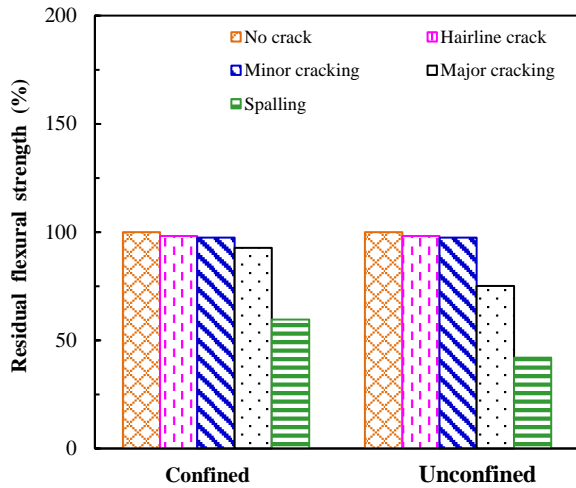


Fig. 9 Normalised residual flexural strength versus cover surface defects for confined and unconfined concrete

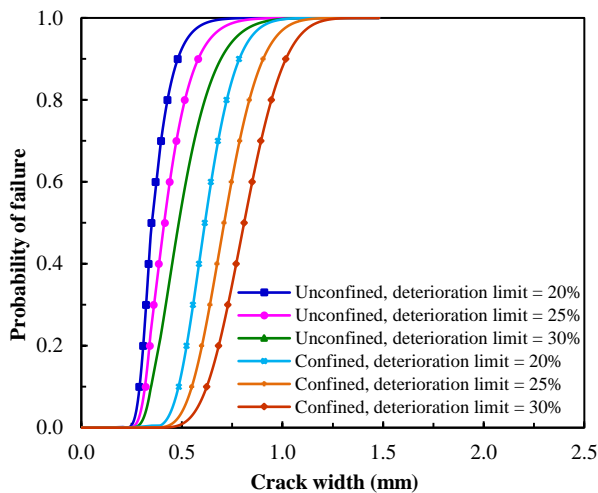


Fig. 10 Probability of failure versus cover surface crack width for various flexural strength deterioration limits of unconfined and confined concrete

crack width, residual flexural strength decreases for all cases, and the deterioration rate is slightly higher in the case with thinner concrete cover.

The influence of different types of aforementioned defects in confined and unconfined concrete is presented in Fig. 9. From the results, at the stage of minor cracking in the concrete cover, there is no significant change in residual flexural strength. As expected, when the defects reach to spalling stage, flexural strength decreases significantly in unconfined concrete.

The probability of failure of the confined and unconfined concrete in terms of flexural strength deterioration is given in Fig. 10 for different allowable flexural strength deterioration limits, i.e., $J_L=20\%$; 25% and 30% . As expected, as further progress of cover cracking probability of failure increases rapidly for both unconfined and confined concrete, showing higher probability of failure for a lower allowable deterioration limit. Furthermore, from the results in Fig. 10, it is clear that the unconfined concrete has considerably lower structural reliability than the

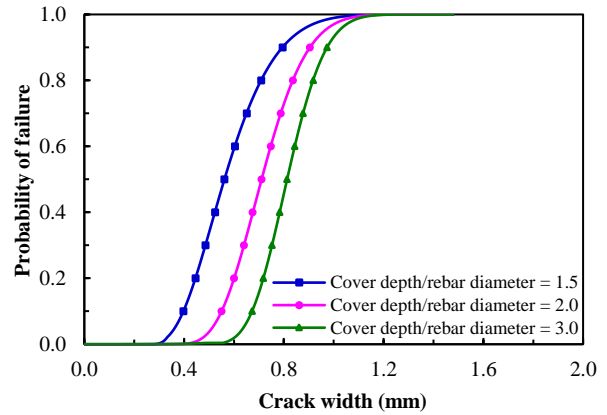


Fig. 11 Probability of failure versus cover surface crack width for various concrete cover depths of confined concrete

confined concrete, when the same predefined allowable limit and concrete cover crack width are considered.

The effect of cover depth on lifecycle performance of confined concrete with respect to flexural strength deterioration is presented in Fig. 11. Here, various cover depths to rebar diameter ratio, e.g., 1.5; 2 and 3, and allowable flexural strength deterioration limit of 25% are considered. The probability of failure increases continuously in all cases of cover depths and reaches to unity when crack width is about 1.2 mm. As expected, the results indicate that the probability of failure is relatively higher in the case of lower cover depth, and the structural failure starts at the early stage of cover surface cracking.

5. Conclusions

In this study, the structural resistance deterioration, such as residual bond strength and load bearing capacity, caused by reinforcement corrosion is investigated. A stochastic deterioration model is then employed to evaluate the failure probability of the corroded RC beam during the service life. The results for the flexural strength deterioration due to reinforcement corrosion are then examined by the experimental and field data available from various sources.

On the basis of the results from the worked examples involving a case study of Ullasund Bridge and RC beam subject to reinforcement corrosion, the following conclusions are drawn: 1) The proposed approach is capable of evaluating the lifecycle performance deterioration of concrete structures subjected to reinforcement corrosion; 2) Flexural strength decreases significantly after critical corrosion level due to significant reduction in bond strength loss. Further progress of corrosion causes significant reduction in rebar size which in turn widens the crack in concrete cover, and consequently reduces both residual bond and flexural strength; 3) The proposed stochastic deterioration model based on the gamma process can effectively assess the structural reliability and the failure probability of corrosion affected RC structures, depending on many factors such as predefined allowable limit of deterioration, concrete cover depth and confinement of the

concrete. The reliability of the corroded structure decreases with the progress of corrosion induced cracking in concrete.

References

- Au, F.T.K. and Du, J.S. (2004), "Prediction of ultimate stress in un-bonded prestressed tendons", *Mag. Concrete Res.*, **56**(1), 1-11.
- Azad, A.K., Ahmad, S. and Al-Gohi, B.H.A. (2010), "Flexural strength of corroded reinforced concrete beams", *Mag. Concrete Res.*, **62**(6), 405-414.
- Azad, A.K., Ahmad, S. and Azher, S.A. (2007), "Residual strength of corrosion-damaged reinforced concrete beams", *ACI Mater. J.*, **104**(1), 40-47.
- Broomfield, J. (1997), *Corrosion of Steel in Concrete: Understanding, Investigating and Repair*, E & FN Spon, London, U.K.
- Cairns, J. and Zhao, Z. (1993), "Behaviour of concrete beams with exposed reinforcement", *Proceedings of the ICE, Structures and Buildings*, **99**(2), 141-154.
- CEB-FIP, CEB-FIP Model Code 1990 (1990), *Design Code*, Thomas Telford, London, U.K.
- Chen, H.P. and Xiao, N. (2012), "Analytical solutions for corrosion-induced cohesive concrete cracking", *J. Appl. Math.*
- Chen, H.P. (2016), "Monitoring based reliability analysis of aging concrete structures by Bayesian updating", *J. Aerosp. Eng.*, B4015004-1-8.
- Chen, H.P. and Alani, A.M. (2012), "Reliability and optimised maintenance for sea defences", *Proceedings of the ICE, Marit. Eng.*, **165**(2), 51-64.
- Chen, H.P. and Alani, A.M. (2013), "Optimized maintenance strategy for concrete structures affected by cracking due to reinforcement corrosion", *ACI Struct. J.*, **110**(2), 229-238.
- Chen, H.P. and Nepal, J. (2015), "Stochastic modelling and lifecycle performance assessment of bond strength of corroded reinforcement in concrete", *Struct. Eng. Mech.*, **54**(2), 319-336.
- Chen, H.P. and Nepal, J. (2016), "Analytical model for residual bond strength of corroded reinforcement in concrete structures", *J. Eng. Mech.*, **142**(2), 04015079-1-8.
- Chung, L., Najm, H. and Balaguru, P. (2008), "Flexural behavior of concrete slabs with corroded bars", *Cement Concrete Compos.*, **30**(3), 184-193.
- Coronelli, D. (2002), "Corrosion cracking and bond strength modelling for corroded bars in reinforced concrete", *ACI Struct. J.*, **99**(3), 267-276.
- Coronelli, D. and Gambarova, P.G. (2000), "A mechanical model for bond strength of corroded reinforcement in concrete", *Proceedings of the 14th Engineering Mechanics Conference*, Austin, Texas, U.S.A.
- Du, Y.G., Clark, L.A. and Chan, A.H.C. (2005), "Residual capacity of corroded reinforcing bars", *Mag. Concrete Res.*, **57**(3), 135-147.
- Eurocode 2 (2004), *Design of Concrete Structure*, European Committee for Standardization, Brussels, Belgium.
- Fang, C., Lundgren, K., Chen, L. and Zhu, C. (2004), "Corrosion influence on bond in reinforced concrete", *Cement Concrete Res.*, **34**(11), 2159-2167.
- Giuriani, E., Plizzari, G. and Schumm, C. (1991), "Role of stirrups and residual tensile strength of cracked concrete on bond", *J. Struct. Eng.*, **117**(1), 1-18.
- Horingmoe, G., Saether, I., Antonsen, R. and Arntsen, B. (2007), *Laboratory Investigations of Steel Bar Corrosion in Concrete Background Document SB-3.10*, Sustainable Bridge, Nourt Technology.
- Khan, I., Francois, R. and Castel, A. (2014), "Prediction of reinforcement corrosion using corrosion induced cracks width in corroded reinforced concrete beams", *Cement Concrete Res.*, **56**, 84-96.
- Law, D.W., Tang, D., Molyneaux, T.K.C. and Gravina, R. (2011), "Impact of crack width on bond: Confined and unconfined rebar", *Mater. Struct.*, **44**(7), 1287-1296.
- Mangat, P.S. and Elgarf, M.S. (1999), "Flexural strength of concrete beams with corroding reinforcement", *ACI Struct. J.*, **96**(1), 149-159.
- Nepal, J. and Chen, H.P. (2015), "Risk-based optimum repair planning of corroded reinforced concrete structures", *Struct. Monitor. Mainten.*, **2**(2), 133-143.
- Shang, H.S., Yi, T.H. and Yang, L.S. (2012), "Experimental study on the compressive strength of big mobility concrete with non-destructive testing method", *Adv. Mater. Sci. Eng.*
- Tilly, G.P. and Jacobs, J. (2007), *Concrete Repairs-Performance in Service and Current Practice*, Willoughby Road, IHS BRE Press, U.K.
- Van Noortwijk, J.M. (2009), "A survey of the application of gamma processes in maintenance", *Reliab. Eng. Syst. Safety*, **94**(1), 2-21.
- Vidal, T., Castel, A. and Francois, R. (2004), "Analyzing crack width to predict corrosion in reinforced concrete", *Cement Concrete Res.*, **34**(1), 165-174.
- Wang, X.H. and Liu, X.L. (2010), "Simplified methodology for the evaluation of residual strength of corroded reinforced concrete beams", *J. Perform. Constr. Facilit.*, **24**(2), 108-119.
- Wang, X.H. and Liu, X.L. (2004), "Modelling effects of corrosion on cover cracking and bond in reinforced concrete", *Mag. Concrete Res.*, **56**(4), 191-199.
- Yalciner, H., Eren, O. and Sensoy, S. (2012), "An experimental study on the bond strength between reinforcement bars and concrete as a function of concrete cover strength and corrosion level", *Cement Concrete Res.*, **42**, 643-655.
- Yi, T.H., Li, H.N. and Wang, C.W. (2016), "Multiaxial sensor placement optimization in structural health monitoring using distributed wolf algorithm", *Struct. Contr. Health Monitor.*, **23**(4), 719-734.
- Zhang, R., Castel, A. and François, R. (2010), "Concrete cover cracking with reinforcement corrosion of RC beam during chloride-induced corrosion process", *Cement Concrete Res.*, **40**(3), 415-425.
- Zhao, Y., Lin, H., Wu, K. and Jin, W. (2013), "Bond behaviour of normal/recycled concrete and corroded steel bars", *Constr. Build. Mater.*, **48**, 348-359.

HK